

Jesus Blanco, Jose L. Fernandez, Angel F. Doval, Carlos Lopez, Francisco Pino and Mariano Perez-Amor "Study of plate vibrations by moire holography," Proc. SPIE 1508, "Industrial Applications of Holographic and Speckle Measuring Techniques," 180-190 (1 October 1991)

Copyright 1991 Society of Photo-Optical Instrumentation Engineers.

This paper was published in "Proceedings of SPIE" and is made available as an electronic reprint with permission of SPIE. One print or electronic copy may be made for personal use only. Systematic or multiple reproduction, distribution to multiple locations via electronic or other means, duplication of any material in this paper for a fee or for commercial purposes, or modification of the content of the paper are prohibited.

<http://dx.doi.org/10.1117/12.47105>

PROCEEDINGS OF SPIE

[SPIDigitalLibrary.org/conference-proceedings-of-spie](https://spiedigitallibrary.org/conference-proceedings-of-spie)

Study of plate vibrations by moire holography

Jesus Blanco-Garcia, J. L. Fernandez, Angel F. Doval, Jose Carlos Lopez Vazquez, Francisco Pino Alvarez, et al.

Jesus Blanco-Garcia, J. L. Fernandez, Angel F. Doval, Jose Carlos Lopez Vazquez, Francisco Pino Alvarez, Mariano Perez-Amor, "Study of plate vibrations by moire holography," Proc. SPIE 1508, Industrial Applications of Holographic and Speckle Measuring Techniques, (1 October 1991); doi: 10.1117/12.47105

SPIE.

Event: ECO4 (The Hague '91), 1991, The Hague, Netherlands

Study of Plate Vibrations by Moiré Holography

J. Blanco
J.L. Fernández
A.F. Doval
C. López
F. Pino
M. Pérez-Amor

Universidad de Vigo, Departamento de Física Aplicada
Lagoas-Marcosende s/n, Vigo, Spain

ABSTRACT

Advantages of moiré holography with single illumination beam as a real-time method to detect vibrational modes of diffusing objects have been already experimentally demonstrated by several authors. The main obstacle to automatize the analysis of the moiré pattern is the difficulty to filter the carrier pattern. At the present it seems affordable to realize that filtering in quasi-real time by means of a digital image-processing system. However, several problems arise in this operation, for example the spread of the spatial frequency spectrum of the carrier fringes. Different filtering algorithms, with and without FFT, are compared. Moreover different ways to combine both carriers are examined.

1. INTRODUCTION

Application of many optical techniques to metrological and nondestructive testing (NDT) tasks leads to the obtaining of fringe patterns that carry information about the magnitude to be measured, allowing to study its variation simultaneously along the whole field of view. This is the case of techniques like classical interferometry, holographic interferometry, photoelasticity, ESPI, shadow and projection moiré, etc.

In the last decade a considerable effort has been done for the development and practical implantation of moiré evaluation methods of fringe patterns due to their high metrological power along with their ability to a real-time operation.¹⁻⁵ One of the applications where the introduction of moiré evaluation methods results more advantageous is the real-time study of mechanical vibrations by holographic interferometry. As it has been already shown,⁶ the use of the "differential moiré" technique in combination with amplitude and phase modulation of the wavefronts in synchronism with the object vibration allows to overcome many of the problems frequently encountered in the practical field work, far from the ideal laboratory conditions (environmental noise: seismic and acoustical, humidity and temperature gradients, dust, object rigid-body movements and global deformations and other effects).

The final step of this technique consists in filtering the carrier fringes from which the moiré pattern -containing the vibration modes information- is formed, in order to allow not only a better visual judgement but also to automate the data acquisition by some fringe-analysis computerized system. Several approaches exist to perform that filtering: optical signal processing,¹ electronic video signal processing or digital image processing. If the system is provided with automatic fringe analysis capability, a frame grabber and a digital processing computer will be usually needed. In this case it seems advantageous to employ this same equipment for digital filtering of the carrier fringes previously to the automatic moiré fringe analysis. In this work we compare different ways to perform the carrier filtering by digital image processing with the aim to reach quasi-real-time operation with maximum flexibility at a minimum cost, making the moiré holography even more attractive and suitable for industrial applications.

2. PRINCIPLE OF THE TECHNIQUE

A moiré pattern gives the difference of pitch between two primary patterns. In moiré holography with single illuminating beam⁶ a carrier pattern is generated on the surface of the object shifting, for example, the illumination source after repositioning. In this case the optical path difference at any point in the object surface may be expressed as

$$D_0 = \vec{d} \cdot \vec{h} \quad (1)$$

where \vec{d} is the shift of the illumination point and \vec{h} an unit vector in the illumination direction. If a deformation of the object takes place, the new path difference is

$$D = \vec{u} \cdot \vec{g} + \vec{d} \cdot \vec{h} \quad (2)$$

where \vec{u} is the object point displacement and \vec{g} is the sensitivity vector.

In the analysis of resonant modes the object is stroboscopically illuminated (two pulses by vibration cycle) after the hologram repositioning. If the exciting frequency is large enough compared to the frame frequency of a video system, two interferograms, each one corresponding to a different state of deformation during an oscillation period, are superimposed in the TV target system and a moiré pattern is formed. The equation of the fringes of each pattern is

$$D_1 = \vec{u}_1 \cdot \vec{g} + \vec{d} \cdot \vec{h} + D_a = n_1 \lambda \quad (3)$$

$$D_2 = \vec{u}_2 \cdot \vec{g} + \vec{d} \cdot \vec{h} + D_a = n_2 \lambda \quad (4)$$

being \vec{u}_1 and \vec{u}_2 the respective object point displacements in each deformation state with respect to the static position (assumed the hologram was recorded with the object at this position), n_1 and n_2 the fringe orders and D_a a time-dependent term due to the ambiental perturbations plus the optical set-up

variations (like repositioning errors). So, the equation of the moiré pattern is

$$D_1 - D_2 = (\vec{u}_1 - \vec{u}_2) \cdot \vec{g} = (n_1 - n_2)\lambda = m\lambda \quad (5)$$

For the validity of eq.(5) several conditions have to be fulfilled:

- 1) As it is usual in holographic interferometry, short displacements of the illumination source and object points have to be assumed. This is necessary in order not only to express the optical path difference due to the object deformation and to the illumination source displacements as $\vec{u} \cdot \vec{g}$ and $\vec{d} \cdot \vec{h}$ respectively but also to ensure that they can be linearly superposed.
- 2) The ambiental perturbation term D_a must have a slow time dependence variation (Fig.1). This variation has to be negligible between two stroboscopic pulses to obtain a moiré pattern in which this term is cancelled. Moreover, as the TV target integrates a certain number of vibration cycles of the object in each frame, the temporal variation of D_a must be small even in a scanning period of the TV camera to avoid the loss of visibility of the moiré pattern.

3. COMPARISON BETWEEN DIFFERENT CARRIER FILTERING ALGORITHMS

Different ways were explored to perform the filtering of the carrier pattern in two steps (Fig.2&3):

- a) the obtaining of the moiré pattern. For this we have considered two possibilities:
 - a.1) the additive moiré formation at the TV target, $A+B$.
 - a.2) the independent acquisition of two carriers, A and B , that can be added, $A+B$, or multiplied, $A \times B$, by the computer.

In any of these cases different operations can be performed in the computer before filtering, leading to images in whose spectra the moiré fringe frequency $|f_A - f_B|$ appears clearly discriminated from the carrier frequencies f_A and f_B .

- b) the proper carrier filtering:
 - b.1) acting on the Fourier plane
 - b.2) acting directly on the image by means of convolutions filters

Among the multiple combinations derived from the above scheme, we have studied the following ones:

- 1) Acquiring each carrier A and B separately and after that manipulating both as follows:
 - 1.1) (AxB). This operation (performed by the computer) gives a quite contrasted image and the moiré frequency $|f_A - f_B|$ is clearly discriminated in the Fourier plane, which allows to filter the carrier by a simple low-pass, (Fig.2). Nevertheless the acquisition of the primary interferograms has to be made with single-pulse stroboscopic illumination and shifting the temporal phase of the amplitude modulation between each acquisition. This makes necessary to determine precisely which states are being compared which in his turn is difficult since the moiré is not viewed in real-time. Moreover the influence of ambiantal perturbations between the two acquisitions is generally not negligible and it masks the information of the resulting moiré.
 - 1.2) (A+B). Making the additive moiré presents the same difficulties than 1.1 with the additional disadvantage of the lack of discrimination of the moiré frequency in the Fourier plane, (Fig.2).
- 2) Starting from the additive moiré formed on the TV target with double pulsed stroboscopic illumination, (A+B), (Figs.4&5). This possibility is more adequated to avoid the influence of ambiantal perturbations. However the moiré frequency is not clearly discriminated in the Fourier plane (Fig.2&4) and the moiré pattern can't be obtained only by means of a low-pass filter.

To overcome this problem we have attempted several solutions:

- 2.1) Shifting the frequency of both carriers f_A and f_B in the Fourier plane an amount $|f_A + f_B|/2$ to the center, (Fig.2). Then, the moiré is obtained by a low-pass filter and making after that the square of the result, $\text{FFT-MASK-SHIFT}-(\text{FFT}^{-1})^2$. The main drawback of this process is that, in practice, the frequency spectrum of each carrier is slightly spreaded in the Fourier plane (Fig.4) (due to the fact that the carrier fringes are neither straight nor equispaced lines and their intensity profile is not purely sinusoidal) which makes both the frequency shift, $|f_A + f_B|/2$, and the low-pass filtering inexact.
- 2.2) Subtracting from the original additive moiré, (A+B), the mean value of the intensity, which can be obtained by an electronic blurred of the proper image, (A+B)_{LP}, and making the square of the result a more contrasted image in whose spectrum the moiré frequency results discriminated is obtained, $[(A+B) - (A+B)_{LP}]^2$, (Fig.2&4). Then a low-pass filtering, either in the Fourier plane or in the image plane, by convolution, can be applied, (Figs.2,4&5).
- 2.3) The same as 2.2 but with a major scale factor in the intensity is obtained subtracting from one addition moiré image the same moiré image but with both carriers shifted a phase π , $[(A+B) - (A+B)\pi]^2$, (Figs.2,4&5).

4. EXPERIMENTAL PROCEDURE

The photographs shown in Figs. 4 & 5 correspond to the methods that we consider more practical and precise to perform the carrier filtering, i.e., 2.2 and 2.3 of the paragraph 3. The following experimental conditions should be remarked:

- The two intermediate images, $|(A+B) - (A+B)_{LP} \text{ and } \pi|$, are derived from two different additive moiré primary images, $A+B$, (different carriers and vibrational amplitudes) of the same resonant mode of the membrane. The three images have a size of 512x512 pixels.
- The two final images filtered by Fourier plane techniques (FF) have a reduced size of 256x256 pixels due to the limited memory of the computer we have used. In the upper image the filtering algorithms have been performed over a box taken from the complete picture with the aim to demonstrate the benefits of enlarging the resolution (and memory size) of the image.
- The two final images filtered by convolution (CONV) have a size of 512x512 pixels. The kernel size is 20x20 pixels.
- For the purpose of accelerating the processes, the operation of making the square of the intermediate images has been substituted by taking their absolute values. The results are very similar in any case.

5. CONCLUSIONS

The problem of filtering the carrier fringe pattern in moiré holography by digital image processing was studied.

Although the multiplicative moiré shows the moiré frequency clearly discriminated in its spectrum, the necessity of acquiring separately the two carriers implies a serious disadvantage.

Different methods to process the additive moiré to obtain the moiré frequency discriminated were attempted. It was demonstrated that both the subtraction of the medium intensity level, $(A+B)_{LP}$, or the subtraction of a carrier-shifted image, $(A+B)\pi$, allow to obtain an intermediate image suitable to be low-pass filtered. However, as the first method is nearly insensitive to drifts of the carrier pattern (very usual in practice due to slight changes in the experimental set-up), it is probably the most convenient one.

About the low-pass carrier filtering, two methods were studied: Fourier plane and convolution filtering. In a first analysis both methods seem to present similar capabilities for filtering the carrier, being in general faster the convolution filtering if a moderated-size kernel (typically less than 20x20 pixels) is employed. Even more, it is possible to apply iteratively this filter to improve the smoothness of the image.

The results obtained up to now suggest that to design an optimum process further work must be done taking in account not only the relevant optical parameters (carriers and moiré spatial bandwidths, speckle size) and filtering parameters (mask size in the Fourier plane or, alternatively, kernel size of the convolution filter), but also the time of operation (aiming to a quasi-real-time process) besides economical considerations. All these subjects are currently being studied by our group.

6. ACKNOWLEDGMENTS

The authors wish to express their deep gratitude to Prof. O.D.D. Soares, Univ. Porto (Portugal), for having introduced them, theoretical and experimentally, into the modern optical metrology and, in particular, into the moiré holography techniques.

The authors acknowledge the financial support of Xunta de Galicia (research project XUGA 7050389) and CICYT (research project ROB-402/90).

7. REFERENCES

1. O.D.D. Soares, A.L.V.S. Lage and L.M. Bernardo, "Moiré Evaluation with Fringe Patterns of Interferograms, Holograms, Moirégrams and Specklegrams" in *Optical Metrology*, O.D.D. Soares (Ed), NATO ASI Series, Serie E, n° 131. pp. 393-425, Martinus Nijhoff Publishers, Dordrecht, The Netherlands, 1987.
2. O.D.D. Soares, A.L.V.S. Lage, "Real-time moiré holography", *Proc. SPIE* n° 615, 1986.
3. P.K. Rastogi, P. Jacquot and L. Pflug, "Contrast enhancement in holographic moiré fringes", *Optica Acta*, Vol. 30, n° 8, pp. 1067-1094, 1983.
4. K. Paturski, "Moiré Methods in Interferometry", *Optics and Laser in Engineering*, Vol. 8, pp. 147-170, 1988.
5. C.M. Vest, "Holographic Metrology and Nondestructive Testing. Past and Future" in *Optical Metrology*, O.D.D. Soares (Ed), NATO ASI Series, Serie E, n° 131. pp. 481-496, Martinus Nijhoff Publishers, Dordrecht, The Netherlands, 1987.
6. O.D.D. Soares and J.L. Fernández, "Moiré evaluation Holography", *Proc. SPIE* n° 673, pp. 198-206, 1986.

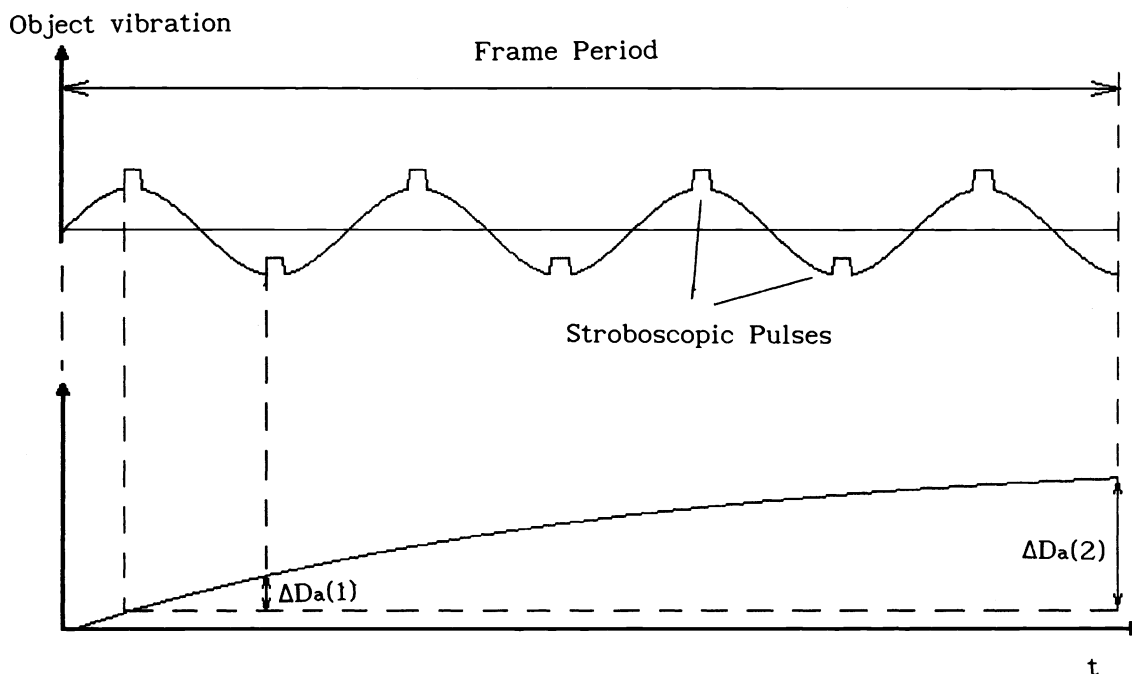


Fig. 1.- A small increment of the perturbation term between two illumination pulses, $\Delta D_a(1)$, less than the admissible error in the amplitude mode measurement is necessary. In addition a small increment of the same term within a frame period, $\Delta D_a(2)$, (typically less than $\pi/2$ in phase) is also required for a good visibility of the moiré pattern.

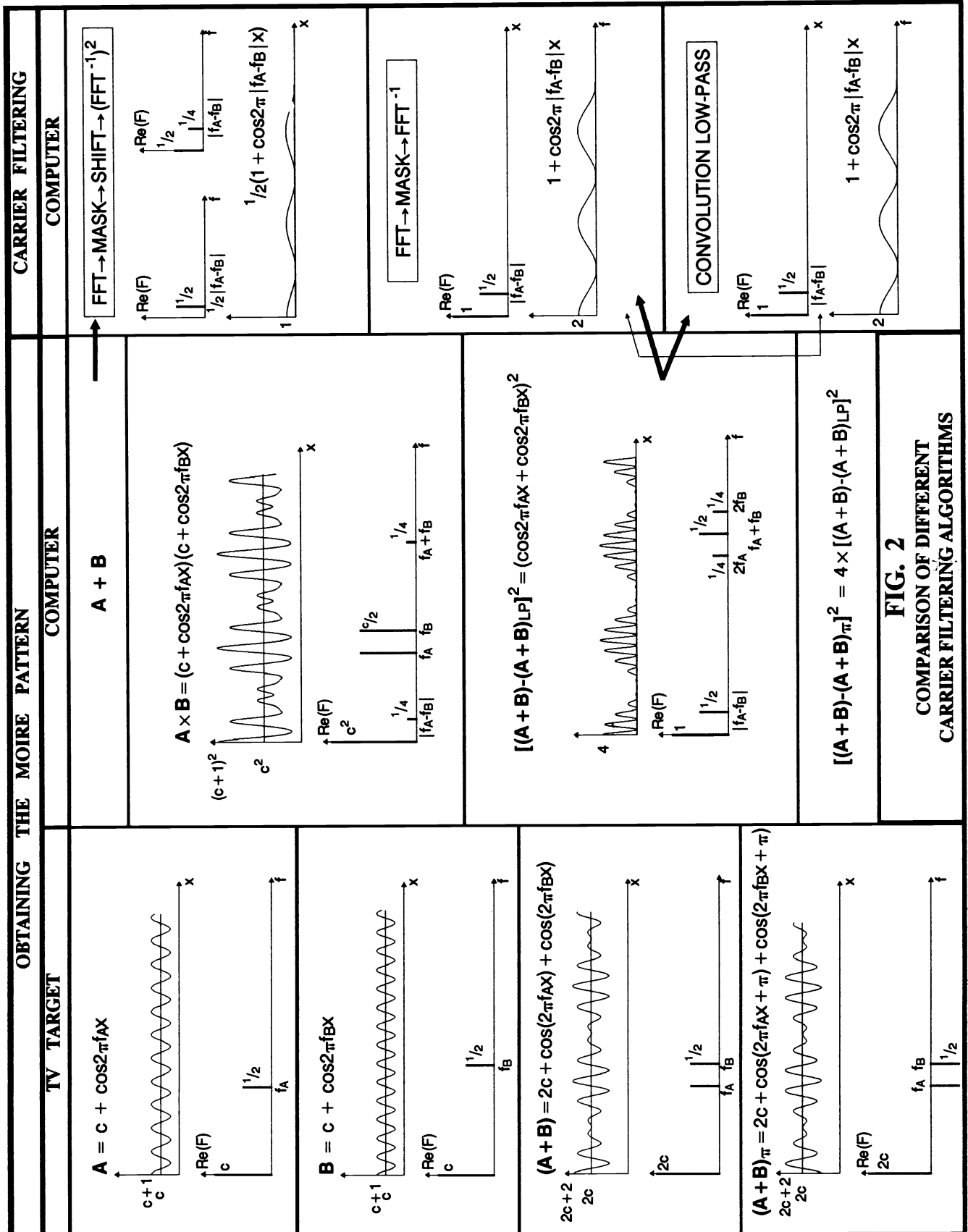


FIG. 2
COMPARISON OF DIFFERENT
CARRIER FILTERING ALGORITHMS

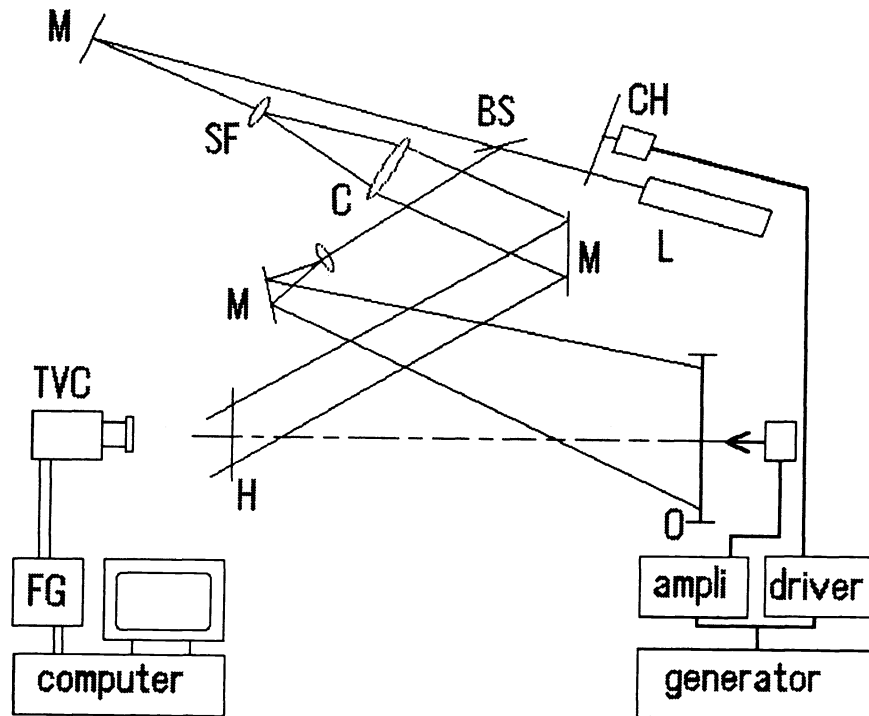


Fig. 3.- Experimental layout. C: collimator; L: laser; SF: spatial filter; M: mirror; BS: beam splitter; O: object; H: hologram plate; CH: chopper; FG: frame grabber; TVC: TV camera.

FIGURES 4 AND 5 CAPTIONS

Fig. 4.- Photographs comparing the four filtering algorithms marked at the bottom of Fig. 2 for a vibrating mebrane in the resonant mode 00. To accelerate the filtering processes, the operation of making the square of the intermediate images, $(A+B) - (A+B)\pi$ and LP, has been substituted by taking their absolute values, rendering very similar results in any case. Fourier transforms (modulus) of the primary, $(A+B)$, and intermediate images are attached. Notation: FF, Fourier plane low-pass filtering, i.e., $FFT \rightarrow MASK \rightarrow FFT^{-1}$; CONV, convolution low-pass filtering. Note that the intermediate images $|(A+B) - (A+B)LP|$ and $|(A+B) - (A+B)\pi|$ have been obtained from two different starting additive moiré images, $(A+B)$, (different carrier fringes and different vibrational amplitudes). In both cases the convolution filter has the same kernel size (20x20 pixels).

Fig. 5.- Photographs illustrating the same filtering algorithms as in Fig. 4 but for the vibration mode 01.

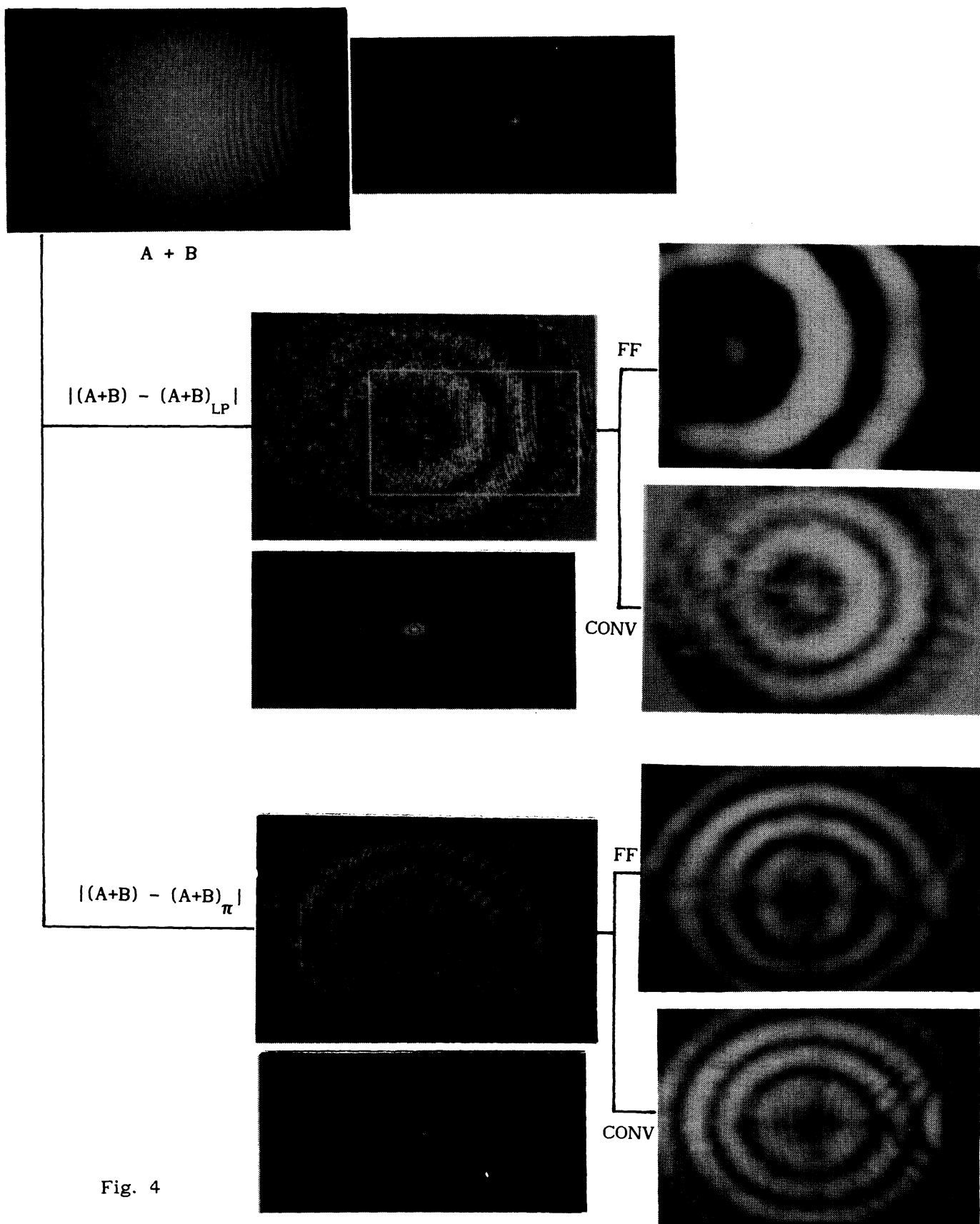


Fig. 4

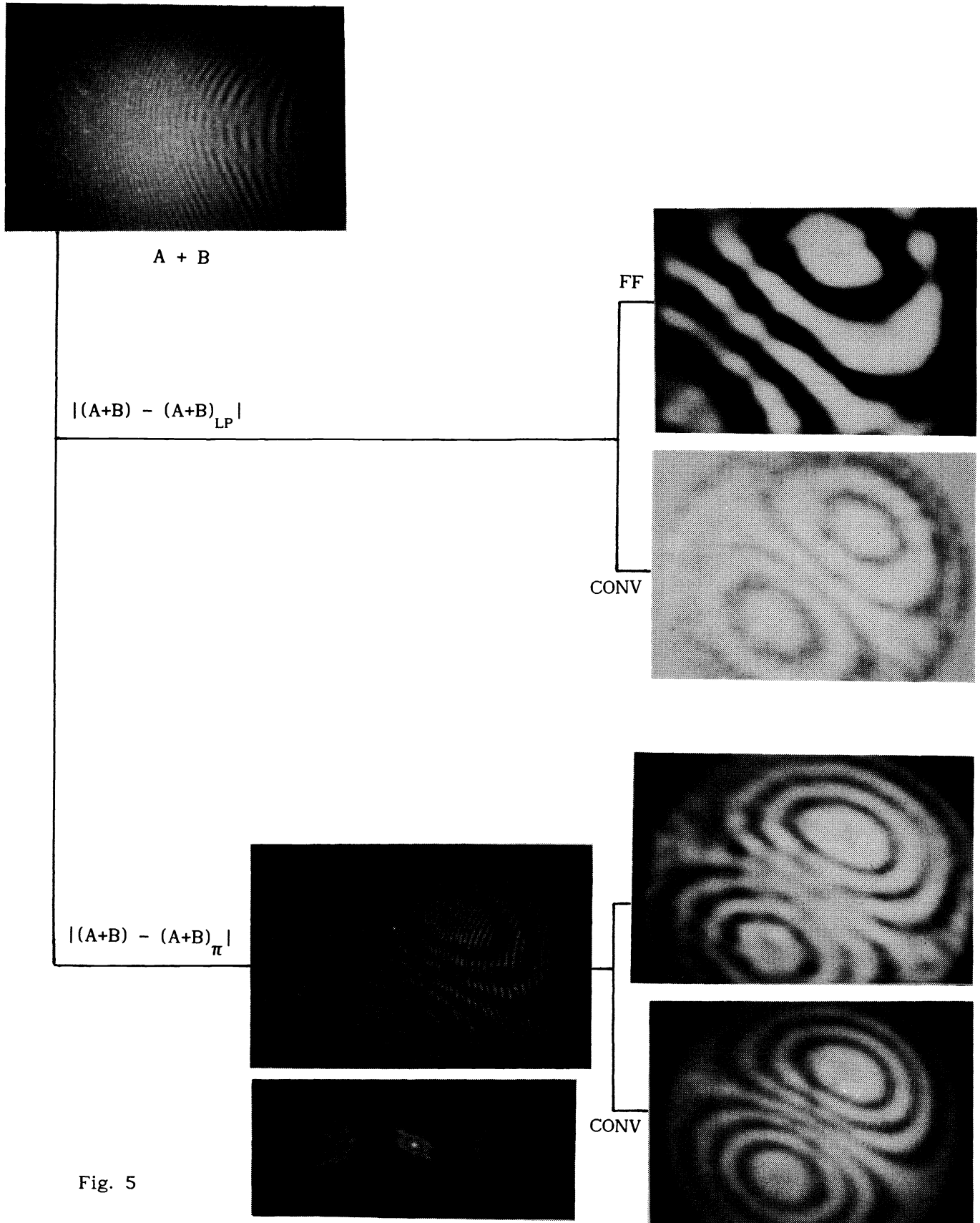


Fig. 5